Abscisic Acid Uridine Diphosphate Glucosyltransferases Play a Crucial Role in Abscisic Acid Homeostasis in Arabidopsis[1][C][W]

Ting Dong, Zheng-Yi Xu, Youngmin Park, Dae Heon Kim, Yongjik Lee, and Inhwan Hwang*

Division of Integrative Biosciences and Biotechnology (T.D., Z.-Y.X., Y.P., Y.L., I.H.) and Department of Life Sciences (D.H.K., I.H.), Pohang University of Science and Technology, Pohang, 790–784 Korea

ORCID ID: 0000-0002-1388-1367 (I.H.).

The phytohormone abscisic acid (ABA) is crucial for plant growth and adaptive responses to various stress conditions. Plants continuously adjust the ABA level to meet physiological needs, but how ABA homeostasis occurs is not fully understood. This study provides evidence that UGT71B6, an ABA uridine diphosphate glucosyltransferase (UGT), and its two closely related homologs, UGT71B7 and UGT71B8, play crucial roles in ABA homeostasis and in adaptation to dehydration, osmotic stress, and high-salinity stresses in Arabidopsis (*Arabidopsis thaliana*). *UGT* RNA interference plants that had low levels of these three *UGT* transcripts displayed hypersensitivity to exogenous ABA and high-salt conditions during germination and exhibited a defect in plant growth. However, the ectopic expression of *UGT71B6* in the *atbg1* (for β-glucosidase) mutant background aggravated the ABA-deficient phenotype of *atbg1* mutant plants. In addition, modulation of the expression of the three *UGTs* affects the expression of *CYP707A1* to *CYP707A4*, which encode ABA 8′-hydroxylases; four *CYP707As* were expressed at higher levels in the *UGT* RNA interference plants but at lower levels in the *UGT71B6*:*GFP*-overexpressing plants. Based on these data, this study proposes that UGT71B6 and its two homologs play a critical role in ABA homeostasis by converting active ABA to an inactive form (abscisic acid-glucose ester) depending on intrinsic cellular and environmental conditions in plants.

The phytohormone abscisic acid (ABA) plays crucial roles in various physiological processes during the plant life cycle, including seed dormancy, germination, stomatal closure, and fruit development (McCarty, 1995; Leung and Giraudat, 1998; Shinozaki and Yamaguchi-Shinozaki, 2000; Himmelbach et al., 2003). The cellular ABA level fluctuates in response to physiological and environmental conditions, and these concentration changes determine ABA function in plant physiology and development (Chernys and Zeevaart, 2000; Wilkinson and Davies, 2002; Zhu, 2002; Leng et al., 2009).

Cellular ABA levels are increased by two different biosynthetic pathways. The primary pathway is the complex de novo synthesis starting from the precursor isopentenyl diphosphate (Zeevaart, 1983; Cutler and Krochko, 1999; Qin and Zeevaart, 1999; Nambara and Marion-Poll, 2005). All steps in the de novo ABA biosynthetic pathway occur in plastids, with the exception of the last two steps that occur in the cytosol (Marin et al., 1996; Tan et al., 1997; Seo and Koshiba, 2002). All reactions in the de novo biosynthetic pathway have been elucidated in detail in various plant species (Marin et al., 1996; Tan et al., 1997; Qin and Zeevaart, 1999; Iuchi et al., 2000; Agrawal et al., 2001). Many mutants in the biosynthetic pathway have been isolated and used to define the exact steps and reaction sequences (Cheng et al., 2002; Xiong et al., 2002). These biosynthetic mutants were instrumental for full analysis and elucidation of the de novo pathway for ABA synthesis. A second biosynthetic pathway is the simple one-step hydrolysis of Glc-conjugated ABA (abscisic acid-glucose ester [ABA-GE]) to ABA by two β-glucosidases, AtBG1 and AtBG2, which localize to the endoplasmic reticulum (ER) and vacuole, respectively (Lee et al., 2006; Xu et al., 2012). Both glucosidases actively increase ABA levels during dehydration and osmotic stress conditions; however, the exact mechanism of their activation differs between the two enzymes. AtBG1 undergoes polymerization into a high-M_r form that has higher enzymatic activity during dehydration stress. By contrast, AtBG2 exists as a high-M_r form during normal conditions, and dehydration stress causes an increase in the AtBG2 level via an unknown mechanism (Lee et al., 2006; Xu et al., 2012).

The cellular ABA level is lowered by the two catabolic pathways, hydroxylation and conjugation (Cutler and Krochko, 1999; Qin and Zeevaart, 1999; Kushiro et al., 2004). Members of the cytochrome P450 family, CYP707A1 to CYP707A4, hydroxylate ABA at the 8′ position to produce unstable 8′-hydroxyl ABA, which is converted to phaseic acid by spontaneous isomerization (Kushiro et al., 2004; Okamoto et al., 2006). The conjugation of ABA with Glc is catalyzed by ABA uridine

[1] This work was supported by the National Research Foundation of the Ministry of Science, ICT and Future Planning, Korea (grant no. 2013070270), and the Ministry of Agriculture, Foods and Forestry, Korea (grant no. 609004–05–5–SB240).

* Address correspondence to ihhwang@postech.ac.kr.

The author responsible for distribution of materials integral to the findings presented in this article in accordance with the policy described in the Instructions for Authors (www.plantphysiol.org) is: Inhwan Hwang (ihhwang@postech.ac.kr).

[C] Some figures in this article are displayed in color online but in black and white in the print edition.

[W] The online version of this article contains Web-only data.

www.plantphysiol.org/cgi/doi/10.1104/pp.114.239210

diphosphate glucosyltransferase (UGT) to produce ABA-GE (Xu et al., 2002; Priest et al., 2006). The two catabolic pathways of hydroxylation and conjugation may differ in their consequences for plant physiology. Hydroxylation of ABA by CYP707As to produce 8′-hydroxyl ABA leads to irreversible degradation of ABA, whereas the conjugation of ABA with Glc to produce ABA-GE retains a metabolite that can be converted back to ABA by the hydrolytic activity of AtBG1 and AtBG2 (Lee et al., 2006; Xu et al., 2012). Thus, the conjugation catabolic pathway can be considered as part of the rapid ABA biosynthetic pathway through the function of AtBG1 and AtBG2.

The cellular ABA level in plant cells is regulated by the two opposing biosynthetic and catabolic pathways. The fine-tuning of both pathways is crucial for balancing the cellular ABA level. Although extensive knowledge of the biosynthetic pathways has been obtained by intensive work, the catabolic pathways are still not fully understood. In particular, despite the fact that the conjugation pathway can inactivate ABA and thereby lower the cellular ABA level, its contribution to the fine-tuning of the cellular ABA level is less clear. In Arabidopsis (*Arabidopsis thaliana*), ABA-GE is produced by UGT71B6, an ABA UGT that shows a strict preference for the naturally occurring (+)-ABA enantiomer (Lim et al., 2005). Overexpression of *UGT71B6* in planta increases enzyme activity in leaf extracts that can glucosylate ABA in vitro (Priest et al., 2006). However, overexpression of *UGT71B6* in Arabidopsis does not cause a significant ABA-deficient phenotype. By contrast, overexpression of *CYP707A3* significantly lowers the cellular ABA levels and results in a clear ABA-deficient phenotype (Umezawa et al., 2006). This suggests that hydroxylation is the major pathway for ABA inactivation in plant cells.

In this study, we investigated the role of UGT71B6 in ABA homeostasis. In Arabidopsis, UGT71B6 belongs to one of the UGT subfamilies with multiple, closely related homologs. We provide evidence that UGT71B6 and its two homologs, named UGT71B7 and UGT71B8, modulate the ABA level in vivo and play important roles in plant cell responses to dehydration and osmotic stress and in plant germination and growth. The expression of these three *UGTs* is inversely correlated with the expression of four *CYP707As*. These interactions facilitate the fine-tuning of ABA levels in plant cells.

RESULTS

UGT71B6 and Its Two Closely Related Homologs, UGT71B7 and UGT71B8, Lower Cellular ABA Levels

Arabidopsis UGTs represent a superfamily containing more than 100 homologs (Ross et al., 2001; Lorenc-Kukuła et al., 2004; Yonekura-Sakakibara and Hanada, 2011). Phylogenetic analysis reveals that the Arabidopsis UGT superfamily can be divided into 12 distinct subgroups (Li et al., 2001). *UGT71B6* is located in group E. Two additional UGT homologs that are in group E with *UGT71B6*, At3g21790 and At3g21800, have more than 90% amino acid sequence similarity to *UGT71B6* (Fig. 1A) and are located immediately upstream and downstream of *UGT71B6* on chromosome 3, respectively. Thus, At3g21790 and At3g21800 were named *UGT71B7* and *UGT71B8*, respectively.

To test whether UGT71B7 and UGT71B8 have similar functions to UGT71B6 with respect to inactivation of ABA, we examined the effect of these genes on the expression of an ABA-responsive gene using protoplasts derived from wild-type Arabidopsis (ecotype Columbia [Col-0]; Yoo et al., 2007). First, we established how *UGT71B6* affects the expression of ABA-responsive genes in protoplasts. For this experiment, we produced a fusion construct containing the firefly luciferase (*LUC*) reporter driven by the ABA-responsive *RD29A* promoter ($RD29A_p$; Ishitani et al., 1997). A second construct containing *UGT71B6* tagged with *GFP* at the C terminus, or containing only *GFP* as a control, was used as an effector. The *LUC* and *UGT71B6* constructs were cotransformed into protoplasts, or *LUC* and *GFP* control, and the transcript level of *LUC* was determined by quantitative real-time (qRT)-PCR. The *LUC* transcripts were significantly reduced when cotransformed with *UGT71B6*, compared with that for the cotransformation of *LUC* with *GFP* as a control effector (Fig. 1B). These results confirm that UGT71B6 reduces cellular ABA levels. Next, we examined the effect of the two UGT homologs, *UGT71B7* and *UGT71B8*, on the expression of *LUC*. When *GFP*-tagged forms of *UGT71B7* and *UGT71B8* were cotransformed with $RD29A_p$:*LUC*, they suppressed the expression of *LUC* as was observed for cotransformation with *UGT71B6*. However, an unrelated UGT, UGT73B1, which belongs to group D (Ross et al., 2001), did not show any noticeable effect on the expression of *LUC* when the *GFP*-tagged form of *UGT73B1* was cotransformed into protoplasts with $RD29A_p$:*LUC* (Fig. 1B). These results indicate that UGT71B7 and UGT71B8 reduce the ABA levels similar to that observed for UGT71B6, thereby resulting in the suppression of $RD29A_p$:*LUC*. In addition, these results suggest that the C-terminal GFP moiety did not affect the activity of UGTs.

These results prompted us to examine if these genes play a role in osmotic stress responses. Therefore, we examined their gene expression under osmotic stress conditions. The expression of *UGT71B6* is induced under high osmotic stress conditions and by the application of exogenous ABA (Priest et al., 2006). To test whether the expression of *UGT71B7* and *UGT71B8* is regulated under these conditions, 2-week-old wild-type plants were treated with 100 μM ABA, 100 mM NaCl, or 300 mM mannitol for 1 h, and total RNA from these plants was used for qRT-PCR analysis. *UGT71B6* was included as a positive control. The transcript levels of these three *UGT* homologs were rapidly induced by ABA, NaCl, and mannitol treatments, albeit at different levels (Fig. 1C). These results indicate that *UGT71B7* and *UGT71B8* are involved in the osmotic stress response.

Next, we examined the spatial expression patterns of these three *UGT* homologs. To quantify the expression level, total RNA was prepared from rosettes, cauline leaves, stems, flowers, siliques, and roots of wild-type

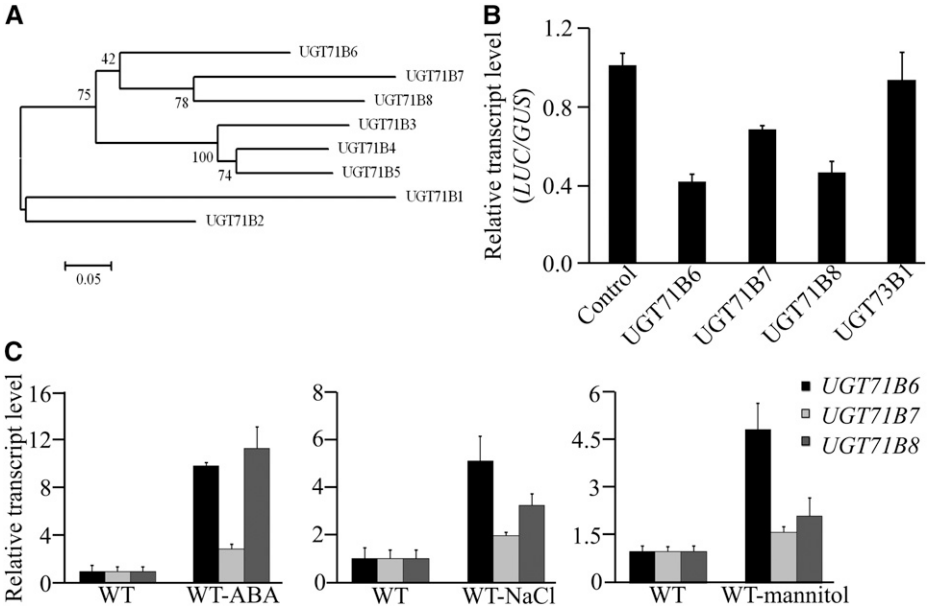

Figure 1. Two *UGT71B6* homologs, *UGT71B7* and *UGT71B8,* reduce the cellular ABA level and are induced by exogenous ABA, NaCl, and osmotic stress. A, Phylogenetic tree of the Arabidopsis UGT71B subfamily. Members were aligned by ClustalW using the default settings for multiple alignments (gap opening of 10; gap extension cost of 0.2; 30% delay for divergent sequences; four-space gap separation distance; without end-gap separation; with residue-specific penalties; and using the Gonnet series protein-weight matrix). The aligned UGT sequences were used to construct a phylogenetic tree with Molecular Evolutionary Genetics Analysis version 5. Distance trees were created using the number of differences. The initial tree was created by maximum likelihood. To estimate the reliability of this tree, bootstrap analysis was performed with 1,000 replicates by using the same weighting parameters as those used in the initial analysis. B, Effects of three *UGTs* on the expression of $RD29A_p$:*LUC* in protoplasts. Protoplasts from wild-type plants were transformed with three plasmids encoding effector, reporter, and normalizer, and the transcript level of the reporter *LUC* was examined by qRT-PCR. *UGT71B6*:*GFP*, *UGT71B7*:*GFP*, *UGT71B8*:*GFP*, and *UGT73B1*:*GFP* were used as effectors; $RD29A_p$:*LUC* was used as a reporter; and $UBQ10_p$:*GUS* was used as a normalizer. *GFP* alone was used as a control for the effector. *GUS* was used as an internal control for qRT-PCR analysis. Error bars indicate SD ($n = 3$). C, Induction of *UGT71B6*, *UGT71B7*, and *UGT71B8* by exogenous ABA, NaCl, and mannitol. Total RNA was prepared from wild-type (WT) plants that had been treated with 100 μM ABA, 100 mM NaCl, or 300 mM mannitol for 1 h and used for qRT-PCR analysis. *ACT2* was used as an internal control. Error bars indicate SD ($n = 3$).

plants and subjected to qRT-PCR analysis. *UGT71B6* was expressed at high levels in rosette and cauline leaves, at low levels in stems, flowers, and siliques, and essentially no expression was detected in root tissues. *UGT71B7* was expressed at high levels in rosette and cauline leaves, flowers, and siliques, at low levels in stems, and essentially no expression was detected in roots. By contrast, *UGT71B8* was strongly expressed only in siliques, with a low level of expression in flowers (Supplemental Fig. S1, A–C). These results indicate that the three *UGTs* showed different spatial and tissue-specific expression patterns. In addition, we also examined the spatial expression patterns of three *UGT* homologs upon abiotic stresses using transgenic plants harboring the *UGT promoter-GUS* constructs. The promoter regions of three *UGTs* were placed upstream of the *GUS* coding region, and transgenic plants harboring these constructs were generated. Two-week-old $UGT71B6_p$:*GUS*, $UGT71B7_p$:*GUS*, and $UGT71B8_p$:*GUS* seedlings were treated with 100 μM ABA or dehydration stress for 3 h. The *GUS* expression in rosette leaves of all three transgenic plants was higher under both ABA and dehydration stress conditions than under the no-stress condition, suggesting that all three *UGTs* are involved in the osmotic stress and drought responses, which is consistent with the data shown in Figure 1C (Supplemental Fig. S1D).

UGT71B6, UGT71B7, and UGT71B8 Are Soluble Proteins That Localize in the Cytosol

To obtain insight into the physiological roles of UGT homologs at the cellular level, we examined their subcellular localizations. We generated transgenic plants expressing the three UGTs tagged with GFP at the C terminus under the control of the 35S promoter. The localization of UGT71B6:GFP, UGT71B7:GFP, and UGT71B8:GFP was examined in protoplasts isolated from these transgenic plants. The GFP fluorescence of all three fusion proteins was observed as a diffuse pattern (Fig. 2A), indicating that they are localized in the cytosol. To verify this result, protein extracts from transgenic plants expressing *UGT71B6*:*GFP*, *UGT71B7*:*GFP*, and *UGT71B8*:*GFP* were separated into soluble

and membrane fractions by ultracentrifugation, and the fractions were analyzed by western blotting using anti-GFP antibody. All three UGTs were detected in soluble fractions (Fig. 2B), which confirms their cytosolic localization. As a control for the soluble fractionation, Arabidopsis aleurain-like protein (AALP; Song et al., 2006) was detected with anti-AALP antibody. It was specifically detected in the soluble fraction, confirming the fractionation.

Suppression of *UGT71B6*, *UGT71B7*, and *UGT71B8* Causes Hypersensitivity to Exogenous ABA and High-Salt Stress during Germination

A previous work showed that *UGT71B6* loss-of-function mutant plants did not display any noticeable phenotype (Priest et al., 2006). When we examined single knockout mutants of *UGT71B7* or *UGT71B8*, they did not show any noticeable phenotype (Supplemental Fig. S2). One possible explanation is a functional redundancy among these three UGTs. It may be necessary to generate double or triple *UGT* mutants to observe any noticeable phenotype. However, the tandem localization of the three genes on chromosome 3 makes it difficult to generate the double or triple knockout mutant plants. As an alternative approach, we generated inducible *UGT* RNA interference (RNAi) transgenic plants using a 450-bp fragment of the highly conserved region (shared among the three *UGTs*) under the control of the dexamethasone (Dex)-inducible promoter (Supplemental Fig. S3A). *UGT* RNAi transgenic plants were generated in the wild-type background; we obtained 23 independent lines at the F4 generation. In *UGT* RNAi line 31 (RNAi-31) and *UGT* RNAi line 42 (RNAi-42), the transcript levels of *UGT71B6*, *UGT71B7*, and *UGT71B8*, but not *UGT73B1* used as a control, were greatly reduced when detected by qRT-PCR (Supplemental Fig. S3B). When continuously exposed to 30 μM Dex, *UGT* RNAi transgenic plants showed multiple phenotypes, such as smaller rosette leaves, shorter roots, and pale green leaves (Fig. 3A; Supplemental Fig. S3C). These phenotypes were observed only in *UGT* RNAi plants but not in *pTA* control plants, confirming that these phenotypes are caused by the suppression of the three *UGTs*.

Glc conjugation to the carboxyl group of (+)-ABA is one of the two catabolic pathways that lower ABA levels (Zeevaart, 1983; Cutler and Krochko, 1999). We determined whether knockdown of *UGT71B6*, *UGT71B7*, and *UGT71B8* affects ABA responses. In these experiments, vector control (VC), RNAi-31, and RNAi-42 seeds were planted on one-half-strength Murashige and Skoog (1/2 MS) plates supplemented with 30 μM Dex, and the germination rate was determined at varying time points. At 4 d after planting, the germination rate of VC seeds was more than 90%, whereas the germination rate of the two independent RNAi seeds was less than 35% (Fig. 3, B and C). When the germination rate was examined on a plate supplemented with 1 μM ABA or 100 mM NaCl in the presence of Dex, the seed germination rate was reduced further; at 4 d after planting, RNAi seeds treated with 100 mM NaCl barely produced any green cotyledons compared with the control seeds, which showed 30% cotyledon greening (Fig. 3D; Supplemental Fig. S4). One possible explanation is that the cellular ABA levels are higher in RNAi seeds than in VC seeds. Next, we examined the ABA-related developmental phenotype of RNAi plants at postgermination stages under different abiotic stress conditions. Transgenic plants of two independent RNAi and VC lines grown on 1/2 MS plates for 5 d were transplanted onto 1/2 MS plates containing 30 μM Dex together with 10 μM ABA or 200 mM mannitol. At 2 weeks after transplantation, plant growth was measured by the primary root length and fresh weight.

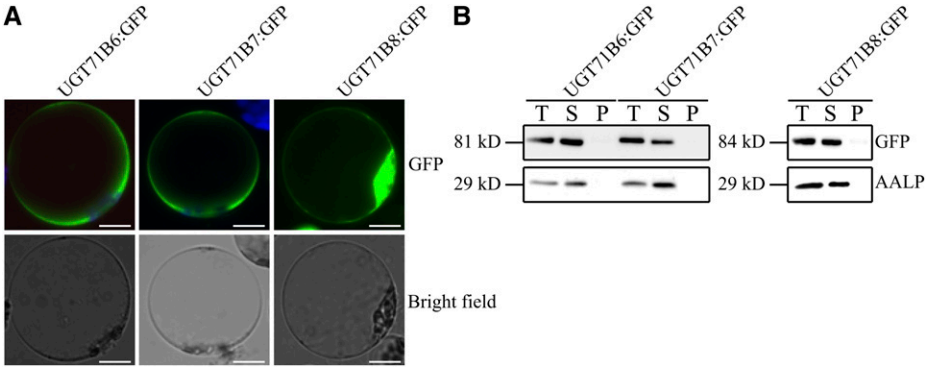

Figure 2. Three GFP-tagged UGT homologs, UGT71B6:GFP, UGT71B7:GFP, and UGT71B8:GFP, are soluble proteins that localize to the cytosol. A, Localization of UGT71B6:GFP, UGT71B7:GFP, and UGT71B8:GFP. Protoplasts from *UGT71B6:GFP*, *UGT71B7:GFP*, and *UGT71B8:GFP* transgenic plants were isolated, and the localization of the proteins was examined. Bars = 20 μm. B, Fractionation of UGT71B6:GFP, UGT71B7:GFP, and UGT71B8:GFP. Protein extracts from plants expressing *UGT71B6:GFP*, *UGT71B7:GFP*, or *UGT71B8:GFP* were separated into soluble and membrane fractions by ultracentrifugation, and these fractions were analyzed by western blotting using anti-GFP antibody. As a control for the fractionation, AALP was detected using anti-AALP antibody. T, Total protein extracts from plants; S, soluble fraction; P, membrane fraction. [See online article for color version of this figure.]

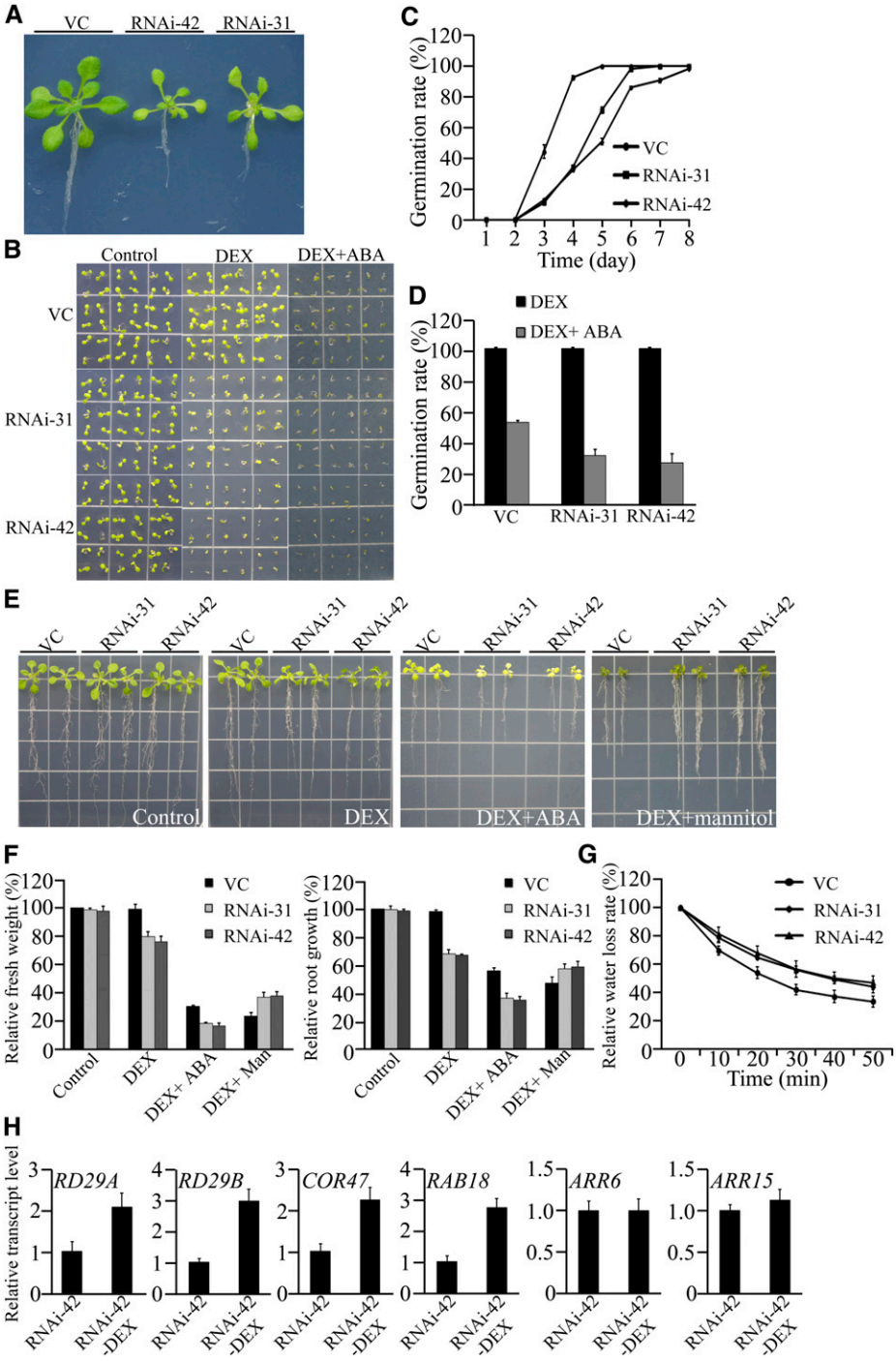

Figure 3. *UGT* RNAi plants display hypersensitivity to exogenous ABA during germination. A, Defect in vegetative growth of RNAi plants. Plants were grown on 1/2 MS plates supplemented with 30 μM Dex. Images were taken 3 weeks after planting. B to D, Germination rates of VC, RNAi-31, and RNAi-42 plants. Seeds were planted on 1/2 MS plates supplemented with 30 μM Dex or with 30 μM Dex and 1 μM ABA. B, Images of germinating plants were taken 7 d after planting. C, Cotyledon emergence was counted at the indicated time points. D, Radicle emergence was counted 4 d after planting. For each type of plant, 50 seeds were used in a triplicate experiment. Error bars indicate SD (n = 3). E and F, Postgermination phenotypes of *UGT* RNAi plants. VC, RNAi-31, and RNAi-42 plants were grown on 1/2 MS plates for 5 d and transferred to 1/2 MS plates supplemented with 30 μM Dex with or without 10 μM ABA or 200 mM mannitol. E, Images were taken 2 weeks after transfer. F, Quantification of the postgermination growth rate. To quantify the growth rate, fresh weight and primary root length were measured 2 weeks after transplantation. Three independent experiments were performed with 20 plants per experiment. Error bars indicate SD (n = 60). G, Water loss of *UGT* RNAi plants. The aerial parts of VC, RNAi-31, and RNAi-42 plants grown on 1/2 MS plates supplemented

The growth rate of RNAi transgenic plants was greatly reduced in the presence of exogenous ABA compared with that of the VC plants. Moreover, RNAi transgenic plants showed higher resistance to mannitol than VC plants (Fig. 3, E and F). These results indicate that *UGT* RNAi transgenic plants are hypersensitive to exogenous ABA and display enhanced resistance to osmotic stress. Next, to assess whether the suppression of all three *UGTs* has any effect on the dehydration stress response, we measured the relative water loss. The aerial parts of VC and RNAi plants were excised, and the rate of water loss was examined under dehydration conditions. RNAi plants lost water more slowly than VC plants, confirming that RNAi plants are more resistant to dehydration stress (Fig. 3G).

To gain insight into the underlying cause of the ABA-hypersensitive phenotype, we examined whether the mode of ABA signaling was affected in RNAi transgenic plants. Total RNA was isolated from 10-d-old RNAi-42 transgenic plants grown in the presence or absence of 30 μM Dex for 10 h, and the expression of the ABA-responsive genes *Responsive to Dessication29A* (*RD29A*), *RD29B*, *Cold Regulated47* (*COR47*), *and Responsive to ABA18* (*RAB18*) and the cytokinin-responsive genes *Type-A Responsive Regulator6* (*ARR6*) and *ARR15* as negative controls was examined by qRT-PCR. The Dex treatment increased the transcript levels of *RD29A*, *RD29B*, *COR47*, and *RAB18* by more than 2-fold, whereas the expression of *ARR6* and *ARR15* was not altered (Fig. 3H). These results confirm that ABA-mediated signaling is specifically activated in *UGT* RNAi plants.

Ectopic Expression of *UGT71B6* Aggravates the ABA-Deficient Phenotype of *atbg1* Mutant Plants

UGT71B6:*GFP*-overexpressing transgenic plants (*UGT71B6*:*GFP*) cause no noticeable ABA-deficient phenotype or only a weakly deficient phenotype (Supplemental Fig. S5; Priest et al., 2006), despite the fact that UGT71B6 can lower the cellular ABA level by converting ABA to ABA-GE. Similar to *UGT71B6*:*GFP* transgenic plants, both *UGT71B7*:*GFP* and *UGT71B8*:*GFP* transgenic plants did not display any noticeable alteration in osmotic and dehydration stress responses compared with wild-type plants except an increase in cotyledon greening in the presence of 6% Glc (Supplemental Fig. S5), indicating that overexpression of *UGTs* has a minor effect on ABA levels. Recent work shows that two β-glucosidases, AtBG1 and AtBG2, which localize to the ER and the vacuole, respectively, can hydrolyze ABA-GE to ABA (Lee et al., 2006; Xu et al., 2012). We questioned if AtBG1 and/or AtBG2 were involved in the lack of an apparent ABA-deficient phenotype in the *UGT71B6*-overexpressing transgenic plants. One possible scenario is that hydrolysis of ABA-GE to ABA by these two β-glucosidases may compensate for the UGT71B6-mediated reduction in ABA levels. To test this, we introduced *UGT71B6*:*GFP* into *atbg1* mutant plants and examined their phenotype. Under normal growth conditions, transgenic plants of two independent lines, 4-3 (*UGT71B6*:*GFP/atbg1-4.3*) and 8-4 (*UGT71B6*:*GFP/atbg1-8.4*), showed a significantly higher germination rate than *atbg1* or wild-type plants (Fig. 4A). The higher germination rate of *UGT71B6*:*GFP*/*atbg1* transgenic plants was more prominent in the presence of 125 or 150 mM NaCl (Fig. 4, B and C). Similarly, *UGT71B6*:*GFP/atbg1-4.3* and *UGT71B6*:*GFP/atbg1-8.4* plants had significantly higher germination rates than *atbg1* and wild-type plants in the presence of 0.5 μM ABA (Supplemental Fig. S6), indicating that the transgenic plants have lower levels of ABA. One possible explanation is that *UGT71B6* overexpression causes a reduction of the cellular ABA level. These results also support the hypothesis that two opposing pathways, conjugation of Glc to ABA by UGT71B6 and hydrolysis of ABA-GE to ABA by AtBG1 and/or AtBG2, contribute to the homeostasis of cellular ABA levels.

To gain further insight into the physiological roles of *UGT71B6*, the aerial parts of wild-type, *UGT71B6*:*GFP*, *atbg1*, and *UGT71B6*:*GFP/atbg1-4.3* plants were excised, and the rate of water loss was examined under dehydration conditions. As observed previously (Lee et al., 2006), *atbg1* plants displayed an increased rate of water loss compared with wild-type and *UGT71B6*:*GFP* plants (Fig. 4D). The rate of water loss in *UGT71B6*:*GFP/atbg1-4.3* mutant plants was higher than that in *UGT71B6*:*GFP* or *atbg1* plants and appeared to be equivalent to the additive effects of both *UGT71B6*:*GFP* and *atbg1* plants. This indicates that *UGT71B6* overexpression causes an additional reduction of ABA levels in the *atbg1* background. To confirm this result, we grew wild-type, *UGT71B6*:*GFP*, *atbg1*, and *UGT71B6*:*GFP/atbg1-4.3* plants for 3 weeks on soil under normal growth conditions, kept the plants in a greenhouse without watering for 10 d, and then started watering again. The survival rate was determined at 2 d after the start of rewatering (Fig. 4, E and F). *UGT71B6*:*GFP/atbg1-4.3* plants were the most sensitive to dehydration stress, followed by *atbg1* plants, indicating that UGT71B6 plays an important role in the cellular response to dehydration stress.

To gain further insight into the function of UGT71B6 in osmotic stress responses, the expression of osmotic

Figure 3. (*Continued.*)
with 30 μM Dex for 2 weeks were excised and exposed to the 30% relative humidity condition for the indicated period of time. To quantify water loss, the weight of the plant tissues was measured at the indicated time points. Error bars indicate SD (n = 30). H, Transcript levels of ABA-inducible genes in *UGT* RNAi transgenic plants. Total RNA was isolated from RNAi-42 transgenic plants treated with or without 30 μM Dex for 10 h, and the ABA-inducible genes *RD29A*, *RD29B*, *COR47*, and *RAB18* were examined by qRT-PCR. The cytokinin-inducible genes *ARR6* and *ARR15* were included as negative controls. *ACT2* was used as an internal control. Error bars indicate SD (n = 3).

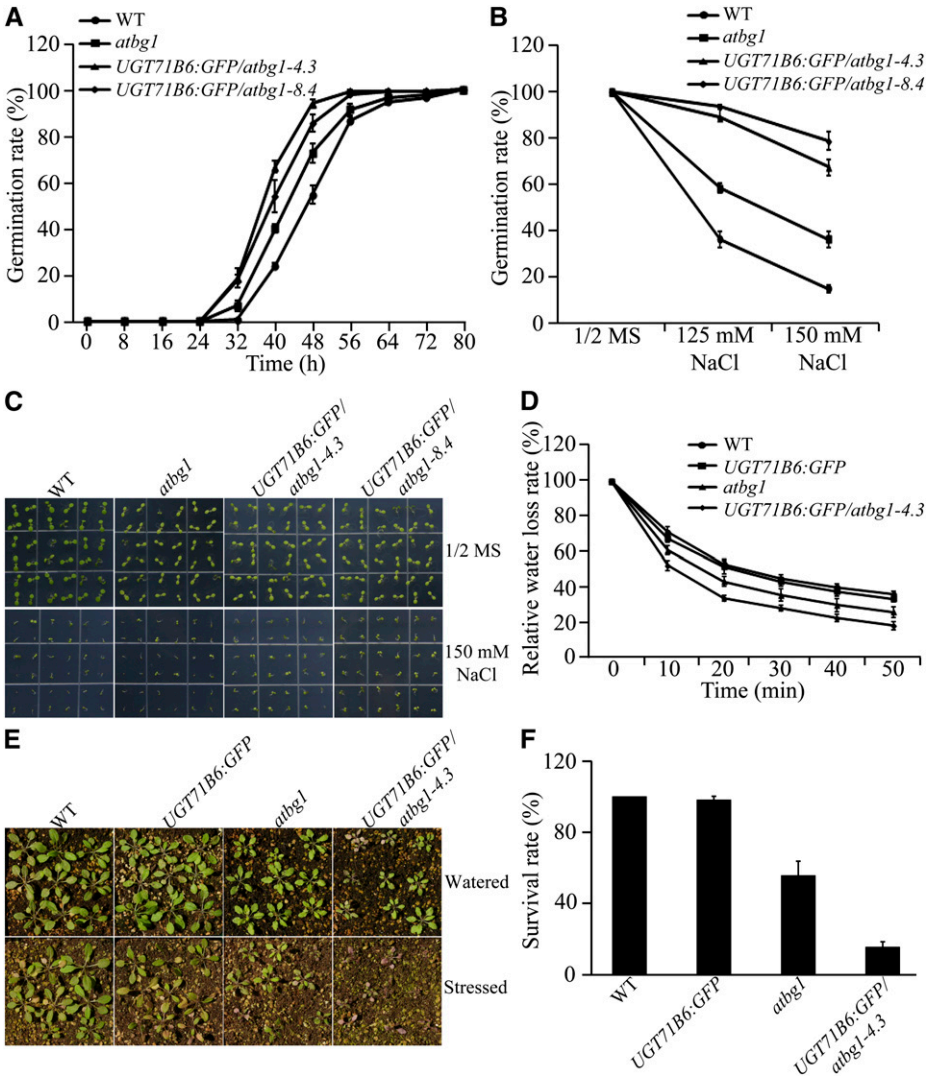

Figure 4. Ectopic expression of *UGT71B6* aggravates the ABA-deficient phenotype of *atbg1* mutant plants. A, Germination rates of wild-type (WT), *atbg1*, *UGT71B6*:*GFP/atbg1-4.3*, and *UGT71B6*:*GFP/atbg1-8.4* seeds. Seeds were planted on 1/2 MS plates, and the germination rate was determined at the indicated time points. For each plant line, 50 seeds were used in a triplicate experiment. Error bars indicate SD ($n = 3$). B, Effects of NaCl stress on germination rates of wild-type, *atbg1*, *UGT71B6*:*GFP/atbg1-4.3*, and *UGT71B6*:*GFP/atbg1-8.4* seeds. Seeds were planted on 1/2 MS plates supplemented with 125 or 150 mM NaCl, and the germination rate was determined 4 d after planting. For each plant line, 50 seeds were used in a triplicate experiment. Error bars indicate SD ($n = 3$). C, Images of germinating seeds were taken 7 d after planting. D, Comparison of water loss among various types of plants. The aerial part of wild-type, *UGT71B6*:*GFP*, *atbg1*, and *UGT71B6*:*GFP/atbg1-4.3* plants grown on 1/2 MS plates for 2 weeks was excised and exposed to the 30% relative humidity condition for the indicated period of time. To quantify water loss, the weight of the plant tissues was measured at the indicated time points. Error bars indicate SD ($n = 20$). E, Dehydration stress sensitivity among various plants. Wild-type, *UGT71B6*:*GFP*, *atbg1*, and *UGT71B6*:*GFP/atbg1-4.3* plants were grown for 3 weeks on soil under normal growth conditions (watered), kept in a greenhouse without watering for 10 d, and then rewatered and grown for an additional 2 d (stressed). F, Quantification of the survival rate after dehydration stress. The survival rate was calculated from the results of five independent experiments. For each type of plant, 36 plants were used at each time. Error bars indicate SD ($n = 5$).

stress-inducible genes was examined in the *UGT71B6*:*GFP/atbg1-4.3* plant. Total RNA from wild-type, *atbg1*, and *UGT71B6*:*GFP/atbg1-4.3* plants that had been treated with or without 300 mM mannitol for 1 h was used for qRT-PCR analysis. *aba3* mutant plants were included as a positive control. In *UGT71B6*:*GFP/atbg1-4.3* plants, the induction of *RD29A*, *RAB18*, and *COR47* by 300 mM mannitol was delayed compared with that in the *atbg1* plants, which, in turn, was delayed compared with the expression in wild-type plants (Fig. 5). These results indicate that overexpression of *UGT71B6* inhibits the expression of osmotic stress-inducible genes under high

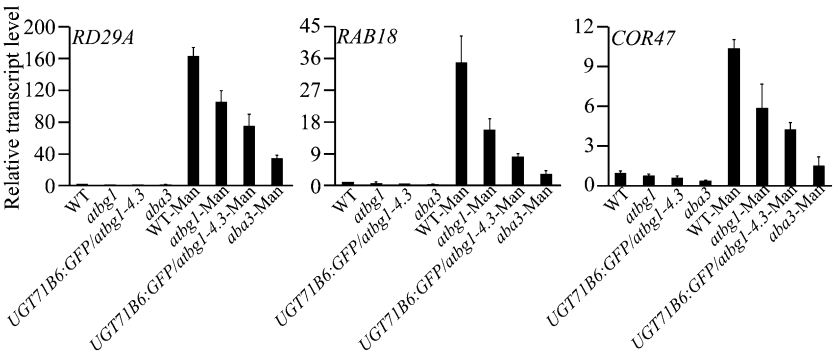

Figure 5. Ectopic expression of *UGT71B6* causes a delay in the induction of osmotic stress-inducible genes. Total RNA was extracted from wild-type (WT), *atbg1*, *UGT71B6*:*GFP/atbg1-4.3*, and *aba3* plants that had been treated for 1 h with or without 300 mM mannitol and used for qRT-PCR analysis. The transcript levels of *RD29A*, *RAB18*, and *COR47* were examined using gene-specific primers. *ACT2* was used as an internal control. Error bars indicate SD ($n = 3$).

osmotic stress conditions. This occurs through a UGT71B6-mediated reduction of the cellular ABA levels.

UGT71B6 Overexpression Reduces the Endogenous ABA Level

To examine the effect of *UGT71B6* overexpression on ABA levels in plants, the ABA content was measured by ELISA using an anti-ABA antibody (Lee et al., 2006). Wild-type, *atbg1*, *UGT71B6*:*GFP/atbg1-4.3*, VC, and RNAi-42 plants were grown on 1/2 MS plates supplemented with or without 30 μM Dex (depending on the induction conditions of the transgenes). *aba3* mutant plants were included as a control. Consistent with the published results (Xiong et al., 2001), ABA contents in the wild-type and *aba3* seedlings were essentially the same under the no-stress condition. However, the ABA content of Dex-treated RNAi-42 plants was 200% that of the Dex-treated VC plants, whereas the ABA contents of *atbg1* and *UGT71B6*:*GFP/atbg1-4.3* plants were only 40% and 25% that of the wild type, respectively (Fig. 6). These results indicate that *UGT71B6*, *UGT71B7*, and *UGT71B8* play important roles to reduce the cellular ABA level. These results are consistent with the phenotypes of these plants (Lee et al., 2006).

Modulation of the *UGT* Homolog Expression Levels Affects ABA Catabolic Genes *CYP707A1* to *CYP707A4*

The cellular ABA levels in plants are also reduced by the hydroxylation pathway. To gain insight into possible interactions between hydroxylation and conjugation catabolic pathways, we examined whether modulation of the expression of *UGT71B6*, *UGT71B7*, and *UGT71B8* affects the expression of four genes, *CYP707A1* to *CYP707A4*, which are involved in the hydroxylation of ABA. VC and RNAi-31 plants grown on 1/2 MS plates supplemented with 30 μM Dex were treated for 1 h with or without dehydration stress, and total RNA from these plants was used for qRT-PCR analysis of the four *CYP70As*. The transcript levels of all four *CYP707As* were significantly higher in RNAi-31 compared with VC plants, both with and without dehydration stress (Fig. 7A). Similarly, upon treatment with salt (100 mM NaCl) and osmotic stress (300 mM mannitol), the transcript levels of all four *CYP707As* were remarkably higher in RNAi-31 than in VC plants, both with or without stress treatment (Fig. 7, B and C). These results indicate that suppression of *UGT* expression induces the expression of *CYP707A1* to *CYP707A4*, which functions to compensate for the loss of the UGT-mediated catabolic pathway. Next, we examined the transcript levels of the four *CYP707As* in *UGT71B6*:*GFP* plants after treatment for 1 h with or without dehydration stress. The transcript levels of the four *CYP707As* were strongly reduced in *UGT71B6*:*GFP* plants (Fig. 8A). Similar results were obtained with salt and osmotic stress treatments (Fig. 8, B and C), indicating that strong expression of *UGT71B6* suppresses *CYP707As*. These results raised the possibility that a regulatory circuit exists to coordinate the opposing expression of genes involved in the two ABA catabolic pathways (Supplemental Figs. S7 and S8).

DISCUSSION

UGTs glycosylate a broad range of acceptor molecules, including plant hormones and all major classes of plant secondary metabolites, and play an important role in enhancing water solubility and the deactivation or detoxification of natural products (Vogt and Jones,

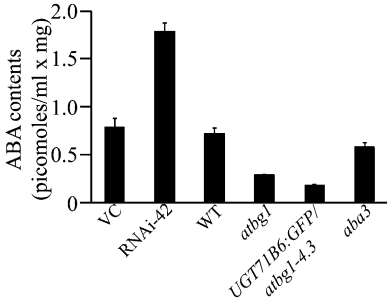

Figure 6. Modulation of *UGT71B6* expression affects the cellular ABA level. VC and RNAi-42 plants were grown on 1/2 MS plates supplemented with 30 μM Dex; wild-type (WT), *atbg1*, *UGT71B6*:*GFP/atbg1-4.3*, and *aba3* plants were grown on 1/2 MS plates. ABA levels were measured by ELISA using anti-ABA antibody. Error bars indicate SD ($n = 3$).

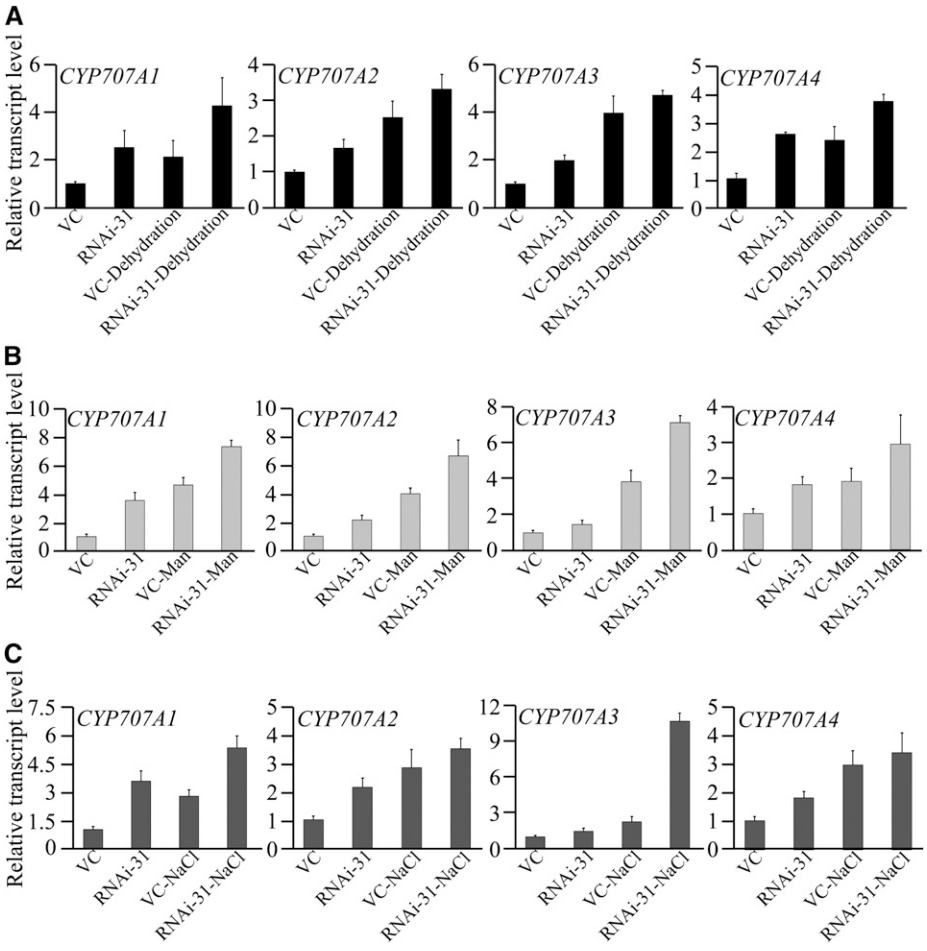

Figure 7. The four ABA hydroxylation genes *CYP707A1* to *CYP707A4* are strongly induced in *UGT* RNAi plants. VC and RNAi-31 plants were grown for 10 d on 1/2 MS plates supplemented with 30 μM Dex and then treated for 1 h with or without dehydration stress (A) or grown in liquid medium for 10 d and treated with 30 μM Dex for 10 h followed by 1 h of treatment of 300 mM mannitol (B) or 100 mM NaCl (C). Total RNA from these plants was used for qRT-PCR analysis of *CYP707A1* to *CYP707A4*. *ACT2* was used as an internal control. Error bars indicate SD (n = 3).

2000; Ross et al., 2001; Yonekura-Sakakibara and Hanada, 2011). Arabidopsis contains a large number of UGTs. UGT71B6 has ABA glucosyltransferase activity that can convert ABA to ABA-GE (Priest et al., 2006). However, its involvement in the regulation of cellular ABA content has not been fully established. The knockout mutant of *UGT71B6* did not give any noticeable phenotype, and *UGT71B6* overexpression had a marginal effect on reducing the ABA content (Priest et al., 2006). By contrast, overexpression of *CYP707A3*, one of four P450 hydroxylases involved in 8′-hydroxylation of ABA in Arabidopsis, significantly reduces endogenous ABA levels (Millar et al., 2006; Umezawa et al., 2006). In this report, we provide evidence that *UGT71B6* and its two closely related homologs, *UGT71B7* and *UGT71B8*, play important roles in modulating cellular ABA levels. This conclusion is based on several lines of experimental evidence. First, ectopic expression of all three *UGTs* (*UGT71B6*, *UGT71B7*, and *UGT71B8*) in protoplasts suppressed the ABA-induced expression of $RD29A_p$:*LUC*, a reporter construct consisting of the ABA-responsive *RD29A* promoter and the *LUC* coding region. Second, *UGT* RNAi transgenic plants showed hypersensitivity to exogenous ABA during germination and post-germination growth, stronger expression of ABA-responsive genes, and a 2-fold increase in cellular ABA levels. Therefore, the lack of any noticeable phenotype in the single knockout mutants *ugt71b6* (Priest et al., 2006), *ugt71b7*, and *ugt71b8* in this study is caused by the functional redundancy among these three genes.

Despite the ABA-related phenotype of the RNAi plants, *UGT71B6* overexpression had a marginal effect on reducing the ABA content (Priest et al., 2006) and produced essentially no observable ABA-deficient phenotype. ABA is produced in plant cells by multiple pathways. Two β-glucosidases use ABA-GE, the product of ABA glucosyltransferase, as a substrate to produce ABA, raising the possibility that a close connection exists in the catabolic and biosynthetic reactions for ABA. A previous study showed that transgenic plants overexpressing *UGT71B6* had higher levels of ABA-GE (Priest et al., 2006). However, the plants showed almost no ABA-deficient phenotype. It is possible that the UGT71B6-mediated reduction of ABA levels is compensated by activation of the AtBG1- and/or AtBG2-mediated ABA synthesis pathways (Lee et al., 2006; Xu et al., 2012). Consistent with this notion, when *UGT71B6* was overexpressed in the *atbg1* background, which is a mutant lacking one of the two ABA-GE hydrolysis pathways, *UGT71B6:GFP/atbg1*

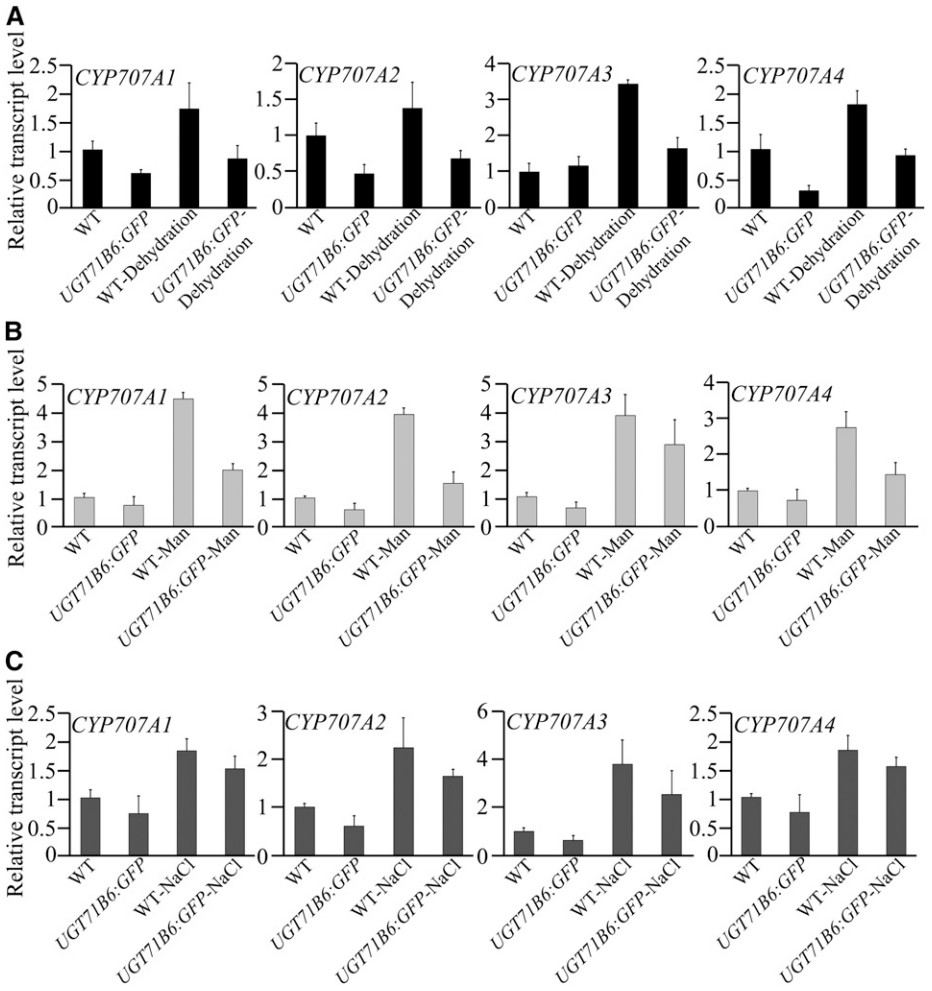

Figure 8. The expression of the four ABA hydroxylation genes *CYP707A1* to *CYP707A4* was significantly suppressed in *UGT71B6:GFP* plants. Wild-type and *UGT71B6:GFP* plants were grown for 10 d on 1/2 MS plates and treated for 1 h with or without dehydration stress (A) or grown in liquid medium for 10 d and treated with 300 mM mannitol (B) or 100 mM NaCl (C) for 1 h. Total RNA from these plants was used for qRT-PCR of the four *CYP707As*. *ACT2* was used as an internal control. Error bars indicate SD ($n = 3$).

plants showed more severe ABA-deficient phenotypes than *UGT71B6:GFP* or *atbg1* plants. Thus, it is likely that the higher level of ABA-GE in *UGT71B6*-overexpressing plants may result in an increase in ABA production through AtBG1- and/or AtBG2-mediated ABA-GE hydrolysis.

In plants, ABA-GE is stored in the vacuole and apoplastic space (Dietz et al., 2000), whereas AtBG1 localizes to the ER (Lee et al., 2006), suggesting that ABA-GE should be imported into the ER. Dehydration stress may act as a signal to transport ABA-GE to the ER via the ER membrane (Lee et al., 2006). This pathway may be under fine control to meet the plant requirement for ABA, as AtBG1 and its substrate ABA-GE are stored separately in the cell and are only brought together when plants need to increase the ABA level upon abiotic stresses. These new findings raise the possibility that a transporter responsible for ABA-GE transport should exist at the ER membrane.

The UGT pathway is one of multiple catabolic pathways for ABA in plant cells. Another important catabolic pathway is the hydroxylation of ABA, which is mediated by four CYP707As, CYP707A1 to CYP707A4. The expression of these *CYP707As* was affected in RNAi or *UGT71B6:GFP* plants. These results raised the possibility that the catabolic pathways are finely coordinated by a certain regulatory circuit at the transcription level. This result is consistent with a previous study showing that an increase in ABA content induces the expression of four *CYP707As* (Kushiro et al., 2004). A similar phenomenon was observed in the *cyp707a1a3* double mutants, which had higher levels of ABA-GE than the wild type (Okamoto et al., 2011). Similarly, the multiple biosynthetic pathways are closely coordinated by a regulatory circuit; the loss of ABA production in the *atbg1* mutant was compensated by the overexpression of *9-CIS-EPOXYCAROTENOID DIOXYGENASE3* or *AtBG2* (Xu et al., 2012).

The ABA levels in plant cells are regulated by the two opposing biosynthetic and catabolic pathways. The biosynthetic and catabolic pathways are localized to multiple organelles. The three UGTs localize in the cytosol. By contrast, CYP707As localize in the ER membrane (Seo and Koshiba, 2011). The localization of enzymes involved in ABA biosynthetic pathways is much more complicated. Most of the de novo biosynthetic enzymes localize

to the chloroplasts, except for the enzymes for the last two steps that occur in the cytosol (Marin et al., 1996; Tan et al., 1997; Seo and Koshiba, 2002). AtBG1 and AtBG2 localize to the ER and vacuole, respectively (Lee et al., 2006; Xu et al., 2012). Therefore, the localization of ABA biosynthetic pathways in multiple organelles raises the intriguing possibility of a complicated regulatory network(s) involving multiple organelles to increase the cellular ABA level. This regulatory network for biosynthetic pathways also needs to be coordinated with catabolic pathways localized in the cytosol and the ER to fine-tune the cellular ABA level. These results shed light on new directions for future work; for example, the role of ABA produced in different compartments, the proportion of the cellular ABA pool produced by any of these individual pathways, and how the ABA levels are coordinated among multiple organelles. It is clear that the compartmentalization of metabolism and signaling plays a critical role in the homeostasis of ABA levels.

In conclusion, we provide evidence that UGT71B6 and its two homologs possess the activity to conjugate Glc to ABA, which reduces ABA levels in plant cells and thereby plays a crucial role in plant growth, development, and adaptive responses. We also propose that the UGT pathway is closely coordinated with the CYP707A pathway for ABA homeostasis in plant cells.

MATERIALS AND METHODS

Plant Growth Conditions

Arabidopsis (*Arabidopsis thaliana*) plants (ecotype Col-0) were grown either on 1/2 MS plates at 20°C in a culture room or in a greenhouse with 70% relative humidity and a 16-h/8-h light/dark cycle at 20°C to 23°C. For NaCl, ABA, or mannitol treatment, plants grown in 1/2 MS liquid medium for 10 d were treated with 100 mM NaCl, 100 μM ABA, or 300 mM mannitol, respectively, for the indicated times as described previously (Piao et al., 1999).

To measure the growth of *UGT* RNAi plants, 5-d-old seedlings grown on 1/2 MS plates containing 1% (w/v) Suc and 0.8% (w/v) agar, pH 5.7, were transferred to 1/2 MS plates supplemented with 30 μM Dex and 10 μM ABA or 200 mM mannitol. Primary root length and fresh weight were measured 2 weeks after transplantation. For growth measurements of transgenic plants overexpressing three *UGTs*, seeds were sown on 1/2 MS plates supplemented with 6% (w/v) Glc or 200 mM mannitol. Cotyledon greening or primary root length was examined after 10 d. For growth measurements of three *UGT* mutant plants, seeds were sown on 1/2 MS plates supplemented with 125 mM NaCl, and the primary root length was examined after 10 d.

To measure relative water loss, the aerial part of plants grown on 1/2 MS plates for 2 weeks was excised and exposed to the dehydration condition for different periods of time. The weight of plant tissues was measured at different time points. For the dehydration stress experiments, 3-week-old plants grown on soil under normal watering conditions were kept in a greenhouse without watering for 10 d. Survival rates were quantified 2 d after rewatering. For the cold stress experiments, 3-week-old plants grown on 1/2 MS plates were incubated at 4°C for different periods of time.

Construction of Plasmids

To generate the *UGT71B6:GFP*, *UGT71B7:GFP*, *UGT71B8:GFP*, and *UGT73B1:GFP* constructs, the complementary DNAs (cDNAs) of *UGT71B6*, *UGT71B7*, *UGT71B8*, and *UGT73B1* were amplified from a Col-0 flower cDNA library by PCR using the gene-specific primers 71B6-5 and 71B6-3, 71B7-5 and 71B7-3, 71B8-5 and 71B8-3, and 73B1-5 and 73B1-3, respectively (for nucleotide sequences of the primers, see Supplemental Table S1), and fused to *GFP* of the 326-GFP vector driven by the 35S promoter (Jin et al., 2001). These constructs were transferred to the binary vector pCsV1300 (Invitrogen) containing the strong cassava vein mosaic virus promoter. The nucleotide sequences of all PCR products were confirmed by sequencing.

To generate the *UGT* RNAi construct, a 450-bp highly conserved region of the three *UGTs* was used. Fragments I and II were amplified by PCR using primers *UGT* RNAi-5 and *UGT* RNAi-3 and *UGT* RNAi-5′ and *UGT* RNAi-3′, respectively, and the products were inserted into the RNAi vector pHANNIBAL using *Bam*HI and *Cla*I sites for fragment I and *Xho*I and *Kpn*I sites for fragment II (Wesley et al., 2001). To generate Dex-inducible transgenic plants, the fragment was inserted into the binary vector pTA7002 using *Xho*I and *Spe*I sites.

To generate *UGT71B6$_p$:GUS*, *UGT71B7$_p$:GUS*, and *UGT71B8$_p$:GUS* constructs, the 441-, 1,833-, and 2,744-bp fragments of the *UGT71B6*, *UGT71B7*, and *UGT71B8* promoter regions were amplified from Col-0 genomic DNA by PCR using the gene-specific primers 71B6-p5 and 71B6-p3, 71B7-p5 and 71B7-p3, and 71B8-p5 and 71B8-p3, respectively, and placed in front of the *GUS* coding region of the binary vector pCAMBIA3301-Bar.

Screening of Arabidopsis Mutants and Reverse Transcription-PCR Analysis of Transcripts

Genomic DNA was prepared from the transfer DNA insertion lines of *ugt71b6* (SALK_001713C), *ugt71b7* (SALK_027837C), and *ugt71b8* (SAIL_75_A08), which were obtained from the Arabidopsis Biological Resource Center. Genotyping was performed using primers UGT71B6-LP and UGT71B6-RP for *ugt71b6*, UGT71B7-LP and UGT71B7-RP for *ugt71b7*, and UGT71B8-LP and UGT71B8-RP for *ugt71b8*.

Total RNA was isolated from leaf tissues of the three *ugt* mutant plants, and the transcript levels of *UGT71B6*, *UGT71B7*, and *UGT71B8* were determined by reverse transcription-PCR using the gene-specific primers 71B6-t5 and 71B6-t3 for *UGT71B6*, 71B7-t5 and 71B7-t3 for *UGT71B7*, and 71B8-t5 and 71B8-t3 for *UGT71B8*. As a control, *18S* ribosomal RNA levels were determined using primers 18S-5 and 18S-3.

Generation of Transgenic Plants

To generate *UGT71B6*-, *UGT71B7*-, and *UGT71B8*-overexpressing transgenic plants, the *UGT71B6:GFP*, *UGT71B7:GFP*, and *UGT71B8:GFP* binary vector constructs were introduced into wild-type plants according to a published protocol (Clough and Bent, 1998). To generate transgenic *atbg1* plants that harbored *UGT71B6:GFP*, the *UGT71B6:GFP* binary vector construct was introduced into *atbg1* mutants. To generate *UGT* RNAi plants, the RNAi binary vector construct was introduced into wild-type plants. pTA7002, the empty vector, was introduced into wild-type plants as a control. These transgenic plants were screened on 1/2 MS plates supplemented with 25 mg L^{-1} hygromycin.

To generate *UGT71B6$_p$:GUS*, *UGT71B7$_p$:GUS*, and *UGT71B8$_p$:GUS* transgenic plants, *UGT71B6$_p$:GUS*, *UGT71B7$_p$:GUS*, and *UGT71B8$_p$:GUS* binary vector constructs were introduced into wild-type plants. Transgenic plants were screened on 1/2 MS plates supplemented with 25 mg L^{-1} DL-phosphinothricin.

Reporter Assay

A suitable amount of plasmids expressing effectors, reporter, and normalizer were cotransformed into protoplasts derived from wild-type plants using the polyethylene glycol transformation method (Jin et al., 2001) and incubated for 20 h at room temperature, and total RNA was extracted from the transformed protoplasts. The transcript levels of *LUC* were detected by qRT-PCR. *GUS* was used as an internal control. Primers were as follows: LUC-5 and LUC-3 for *LUC* and GUS-5 and GUS-3 for *GUS*.

Germination Assay

To measure the germination rate, seeds were harvested and stored under identical conditions. Seeds were surface sterilized, stored at 4°C in the dark for 48 h, planted on 1/2 MS plates containing 1% (w/v) Suc and 0.8% (w/v) agar, and germinated at 22°C in a 16-h/8-h light/dark condition. For ABA or NaCl treatments, the appropriate amounts of ABA or NaCl were supplemented to the 1/2 MS medium.

qRT-Reverse Transcription-PCR

Total RNA was extracted from plants using the Qiagen RNeasy Plant Mini Kit and digested with TURBO DNase (Ambion). Extracted RNA was reverse transcribed to cDNA using the High Capacity cDNA Reverse Transcription Kit (Applied Biosystems). qRT-PCR was performed using the SYBR Green Kit (Applied Biosystems) to detect transcript levels of genes. *ACTIN2* (*ACT2*) was used as an internal control.

Primers used were as follows: 71B6-q5 and 71B6-q3 for *UGT71B6*, 71B7-q5 and 71B7-q3 for *UGT71B7*, 71B8-q5 and 71B8-q3 for *UGT71B8*, 73B1-q5 and 73B1-q3 for *UGT73B1*, ACT2-5 and ACT2-3 for *ACT2*, RD29A-5 and RD29A-3 for *RD29A*, RD29B-5 and RD29B-3 for *RD29B*, COR47-5 and COR47-3 for *COR47*, RAB18-5 and RAB18-3 for *RAB18*, CYP707A1-5 and CYP707A1-3 for *CYP707A1*, CYP707A2-5 and CYP707A2-3 for *CYP707A2*, CYP707A3-5 and CYP707A3-3 for *CYP707A3*, CYP707A4-5 and CYP707A4-3 for *CYP707A4*, BG1-5 and BG1-3 for *AtBG1*, BG2-5 and BG2-3 for *AtBG2*, ARR6-5 and ARR6-3 for *ARR6*, and ARR15-5 and ARR15-3 for *ARR15*.

In Vivo Localization of UGT71B6, UGT71B7, and UGT71B8 in Protoplasts

To investigate the subcellular localization of the three UGTs, protoplasts were isolated from transgenic plants expressing *UGT71B6:GFP*, *UGT71B7:GFP*, and *UGT71B8:GFP*. The localization was examined by fluorescence microscopy (Jin et al., 2001). Images were processed using Adobe Photoshop and presented in pseudocolor.

Fractionation of UGT71B6:GFP, UGT71B7:GFP, and UGT71B8:GFP

Protoplasts were isolated from transgenic plants expressing *UGT71B6:GFP*, *UGT71B7:GFP*, and *UGT71B8:GFP* and suspended in sonication buffer (20 mM Tris-HCl, 2.5 mM $MgCl_2$, 2 mM EGTA, 1 mM EDTA, and 160 mM NaCl). Protoplasts were disrupted by sonication. After discarding debris, the soluble fractions were subjected to ultracentrifugation at 100,000*g* for 1 h. Proteins from soluble and pellet fractions were collected separately and analyzed by immunoblotting using anti-GFP antibody. Total protein extracts from protoplasts were included. As a control for the fractionation, AALP was detected using anti-AALP antibody.

Measurement of Endogenous ABA Levels

Whole-plant tissues (50 mg) were extracted with 80% (v/v) methanol at 4°C for 3 h. The methanol extracts were centrifuged at 3,000*g* for 10 min to remove debris and dried under vacuum. The powder was dissolved in 50 μL of 1× Tris-buffered saline buffer (25 mM Tris-HCl, 100 mM NaCl, 0.1 mM $MgCl_2$, and 0.3% [w/v] NaN_3). The ABA content was determined by competitive ELISA using an anti-ABA antibody according to the protocol of the Phytodetek ABA Test Kit (Agdia).

Measurement of Chlorophyll *a*/*b* Content

Chlorophyll was extracted from leaf tissues of 2-week-old plants using 50 volumes of 95% (v/v) ethanol for 20 min at 80°C. The amount of chlorophyll was calculated as described previously (Vernon, 1960).

GUS Assay

Two-week-old *UGT71B6*$_p$*:GUS*, *UGT71B7*$_p$*:GUS*, and *UGT71B8*$_p$*:GUS* seedlings were treated with or without 100 μM ABA or dehydration stress for 3 h. Histochemical assay of the GUS activity was conducted as follows. Plant materials were incubated in the staining buffer [100 mM $NaPO_4$, pH 7.0, 5 mM $K_3Fe(CN)_6$, 5 mM $K_4Fe(CN)_6$, 10 mM EDTA, 0.1% (v/v) Triton X-100, and 1 mg mL^{-1} 5-bromo-4-chloro-3-indolyl-β-D-galactopyranoside] at 37°C in the dark for 6 h. The tissue was then rinsed several times with 70% (v/v) ethanol. The samples were examined with an anatomical microscope.

Sequence data from this article can be found in the Arabidopsis Genome Initiative databases under the following accession numbers: *UGT71B6* (At3g21780), *UGT71B7* (At3g21790), *UGT71B8* (At3g21800), *UGT73B1* (At4g34138), *RD29A* (At5g52310), *RD29B* (At5g52300), *COR47* (At1g20440), *RAB18* (At5g66400), *CYP707A1* (At4g19230), *CYP707A2* (At2g29090), *CYP707A3* (At5g45340), *CYP707A4* (At3g19270), *AtBG1* (At1g52400), *AtBG2* (At2g32860), *ARR6* (At5g62920), *ARR15* (At1g74890), and *ACT2* (At3g18780).

Supplemental Data

The following materials are available in the online version of this article.

Supplemental Figure S1. Tissue-specific expression of *UGT71B6*, *UGT71B7*, and *UGT71B8*.

Supplemental Figure S2. Germination and postgermination phenotypes of *ugt71b6*, *ugt71b7*, and *ugt71b8* mutant plants.

Supplemental Figure S3. Phenotypes of *UGT* RNAi plants.

Supplemental Figure S4. *UGT* RNAi plants display hypersensitivity to high-NaCl stress during seed germination.

Supplemental Figure S5. Germination and postgermination phenotypes of *UGT71B6:GFP*, *UGT71B7:GFP*, and *UGT71B8:GFP* plants.

Supplemental Figure S6. Ectopic expression of *UGT71B6* aggravates the ABA-deficient phenotype of *atbg1* plants.

Supplemental Figure S7. Transcript levels of *AtBG1* and *AtBG2* in *UGT* RNAi plants under abiotic stress conditions.

Supplemental Figure S8. Transcript levels of *AtBG1* and *AtBG2* in *UGT71B6:GFP* plants under abiotic stress conditions.

Supplemental Table S1. Sequences of primers used in this study.

Received March 6, 2014; accepted March 20, 2014; published March 27, 2014.

LITERATURE CITED

Agrawal GK, Yamazaki M, Kobayashi M, Hirochika R, Miyao A, Hirochika H (2001) Screening of the rice Viviparous mutants generated by endogenous retrotransposon *Tos17* insertion: tagging of a zeaxanthin epoxidase gene and a novel *OsTATC* gene. Plant Physiol **125:** 1248–1257

Cheng WH, Endo A, Zhou L, Penney J, Chen HC, Arroyo A, Leon P, Nambara E, Asami T, Seo M, et al (2002) A unique short-chain dehydrogenase/reductase in Arabidopsis glucose signaling and abscisic acid biosynthesis and functions. Plant Cell **14:** 2723–2743

Chernys JT, Zeevaart JA (2000) Characterization of the 9-cis-epoxycarotenoid dioxygenase gene family and the regulation of abscisic acid biosynthesis in avocado. Plant Physiol **124:** 343–353

Clough SJ, Bent AF (1998) Floral dip: a simplified method for *Agrobacterium*-mediated transformation of *Arabidopsis thaliana*. Plant J **16:** 735–743

Cutler AJ, Krochko JE (1999) Formation and breakdown of ABA. Trends Plant Sci **4:** 472–478

Dietz KJ, Sauter A, Wichert K, Messdaghi D, Hartung W (2000) Extracellular beta-glucosidase activity in barley involved in the hydrolysis of ABA glucose conjugate in leaves. J Exp Bot **51:** 937–944

Himmelbach A, Yang Y, Grill E (2003) Relay and control of abscisic acid signaling. Curr Opin Plant Biol **6:** 470–479

Ishitani M, Xiong L, Stevenson B, Zhu JK (1997) Genetic analysis of osmotic and cold stress signal transduction in *Arabidopsis*: interactions and convergence of abscisic acid-dependent and abscisic acid-independent pathways. Plant Cell **9:** 1935–1949

Iuchi S, Kobayashi M, Yamaguchi-Shinozaki K, Shinozaki K (2000) A stress-inducible gene for 9-cis-epoxycarotenoid dioxygenase involved in abscisic acid biosynthesis under water stress in drought-tolerant cowpea. Plant Physiol **123:** 553–562

Jin JB, Kim YA, Kim SJ, Lee SH, Kim DH, Cheong GW, Hwang I (2001) A new dynamin-like protein, ADL6, is involved in trafficking from the *trans*-Golgi network to the central vacuole in *Arabidopsis*. Plant Cell **13:** 1511–1526

Kushiro T, Okamoto M, Nakabayashi K, Yamagishi K, Kitamura S, Asami T, Hirai N, Koshiba T, Kamiya Y, Nambara E (2004) The Arabidopsis cytochrome P450 CYP707A encodes ABA 8′-hydroxylases: key enzymes in ABA catabolism. EMBO J **23:** 1647–1656

Lee KH, Piao HL, Kim HY, Choi SM, Jiang F, Hartung W, Hwang I, Kwak JM, Lee IJ, Hwang I (2006) Activation of glucosidase via stress-induced polymerization rapidly increases active pools of abscisic acid. Cell **126:** 1109–1120

Leng P, Zhang GL, Li XX, Wang LH, Zheng ZM (2009) Cloning of 9-*cis*-epoxycarotenoid dioxygenase (NCED) gene encoding a key enzyme during abscisic acid (ABA) biosynthesis and ABA-regulated ethylene production in detached young persimmon calyx. Chin Sci Bull **54:** 2830–2838

Leung J, Giraudat J (1998) Abscisic acid signal transduction. Annu Rev Plant Physiol Plant Mol Biol **49:** 199–222

Li Y, Baldauf S, Lim EK, Bowles DJ (2001) Phylogenetic analysis of the UDP-glycosyltransferase multigene family of *Arabidopsis thaliana*. J Biol Chem **276:** 4338–4343

Lim EK, Doucet CJ, Hou B, Jackson RG, Abrams SR, Bowles DJ (2005) Resolution of (+)-abscisic acid using an *Arabidopsis* glycosyltransferase. Tetrahedron Asymmetry **16:** 143–147

Lorenc-Kukuła K, Korobczak A, Aksamit-Stachurska A, Kostyń K, Lukaszewicz M, Szopa J (2004) Glucosyltransferase: the gene arrangement and enzyme function. Cell Mol Biol Lett **9:** 935–946

Marin E, Nussaume L, Quesada A, Gonneau M, Sotta B, Hugueney P, Frey A, Marion-Poll A (1996) Molecular identification of zeaxanthin epoxidase of Nicotiana plumbaginifolia, a gene involved in abscisic acid biosynthesis and corresponding to the ABA locus of Arabidopsis thaliana. EMBO J **15:** 2331–2342

McCarty DR (1995) Genetic control and integration of maturation and germination pathways in seed development. Annu Rev Plant Physiol Plant Mol Biol **46:** 71–93

Millar AA, Jacobsen JV, Ross JJ, Helliwell CA, Poole AT, Scofield G, Reid JB, Gubler F (2006) Seed dormancy and ABA metabolism in Arabidopsis and barley: the role of ABA 8′-hydroxylase. Plant J **45:** 942–954

Nambara E, Marion-Poll A (2005) Abscisic acid biosynthesis and catabolism. Annu Rev Plant Biol **56:** 165–185

Okamoto M, Kushiro T, Jikumaru Y, Abrams SR, Kamiya Y, Seki M, Nambara E (2011) ABA 9′-hydroxylation is catalyzed by CYP707A in Arabidopsis. Phytochemistry **72:** 717–722

Okamoto M, Kuwahara A, Seo M, Kushiro T, Asami T, Hirai N, Kamiya Y, Koshiba T, Nambara E (2006) CYP707A1 and CYP707A2, which encode abscisic acid 8′-hydroxylases, are indispensable for proper control of seed dormancy and germination in Arabidopsis. Plant Physiol **141:** 97–107

Piao HL, Pih KT, Lim JH, Kang SG, Jin JB, Kim SH, Hwang I (1999) An Arabidopsis *GSK3/shaggy*-like gene that complements yeast salt stress-sensitive mutants is induced by NaCl and abscisic acid. Plant Physiol **119:** 1527–1534

Priest DM, Ambrose SJ, Vaistij FE, Elias L, Higgins GS, Ross ARS, Abrams SR, Bowles DJ (2006) Use of the glucosyltransferase UGT71B6 to disturb abscisic acid homeostasis in *Arabidopsis thaliana*. Plant J **46:** 492–502

Qin XQ, Zeevaart JAD (1999) The 9-*cis*-epoxycarotenoid cleavage reaction is the key regulatory step of abscisic acid biosynthesis in water-stressed bean. Proc Natl Acad Sci USA **96:** 15354–15361

Ross J, Li Y, Lim E, Bowles DJ (2001) Higher plant glycosyltransferases. Genome Biol **2:** 3004.3001–3004.3006

Seo M, Koshiba T (2002) Complex regulation of ABA biosynthesis in plants. Trends Plant Sci **7:** 41–48

Seo M, Koshiba T (2011) Transport of ABA from the site of biosynthesis to the site of action. J Plant Res **124:** 501–507

Shinozaki K, Yamaguchi-Shinozaki K (2000) Molecular responses to dehydration and low temperature: differences and cross-talk between two stress signaling pathways. Curr Opin Plant Biol **3:** 217–223

Song J, Lee MH, Lee GJ, Yoo CM, Hwang I (2006) *Arabidopsis* EPSIN1 plays an important role in vacuolar trafficking of soluble cargo proteins in plant cells via interactions with clathrin, AP-1, VTI11, and VSR1. Plant Cell **18:** 2258–2274

Tan BC, Schwartz SH, Zeevaart JA, McCarty DR (1997) Genetic control of abscisic acid biosynthesis in maize. Proc Natl Acad Sci USA **94:** 12235–12240

Umezawa T, Okamoto M, Kushiro T, Nambara E, Oono Y, Seki M, Kobayashi M, Koshiba T, Kamiya Y, Shinozaki K (2006) CYP707A3, a major ABA 8′-hydroxylase involved in dehydration and rehydration response in *Arabidopsis thaliana*. Plant J **46:** 171–182

Vernon LP (1960) Spectrophotometric determination of chlorophylls and pheophytins in plant extracts. Anal Chem **32:** 1144–1150

Vogt T, Jones P (2000) Glycosyltransferases in plant natural product synthesis: characterization of a supergene family. Trends Plant Sci **5:** 380–386

Wesley SV, Helliwell CA, Smith NA, Wang MB, Rouse DT, Liu Q, Gooding PS, Singh SP, Abbott D, Stoutjesdijk PA, et al (2001) Construct design for efficient, effective and high-throughput gene silencing in plants. Plant J **27:** 581–590

Wilkinson S, Davies WJ (2002) ABA-based chemical signalling: the coordination of responses to stress in plants. Plant Cell Environ **25:** 195–210

Xiong L, Ishitani M, Lee H, Zhu JK (2001) The *Arabidopsis LOS5/ABA3* locus encodes a molybdenum cofactor sulfurase and modulates cold stress- and osmotic stress-responsive gene expression. Plant Cell **13:** 2063–2083

Xiong LM, Lee HJ, Ishitani M, Zhu JK (2002) Regulation of osmotic stress-responsive gene expression by the *LOS6/ABA1* locus in *Arabidopsis*. J Biol Chem **277:** 8588–8596

Xu ZJ, Nakajima M, Suzuki Y, Yamaguchi I (2002) Cloning and characterization of the abscisic acid-specific glucosyltransferase gene from adzuki bean seedlings. Plant Physiol **129:** 1285–1295

Xu ZY, Lee KH, Dong T, Jeong JC, Jin JB, Kanno Y, Kim DH, Kim SY, Seo M, Bressan RA, et al (2012) A vacuolar β-glucosidase homolog that possesses glucose-conjugated abscisic acid hydrolyzing activity plays an important role in osmotic stress responses in *Arabidopsis*. Plant Cell **24:** 2184–2199

Yonekura-Sakakibara K, Hanada K (2011) An evolutionary view of functional diversity in family 1 glycosyltransferases. Plant J **66:** 182–193

Yoo SD, Cho YH, Sheen J (2007) *Arabidopsis* mesophyll protoplasts: a versatile cell system for transient gene expression analysis. Nat Protoc **2:** 1565–1572

Zeevaart JA (1983) Metabolism of abscisic acid and its regulation in *Xanthium* leaves during and after water stress. Plant Physiol **71:** 477–481

Zhu JK (2002) Salt and drought stress signal transduction in plants. Annu Rev Plant Biol **53:** 247–273